

Stoner Gap in the Superconducting Ferromagnet UGe₂

N. Aso,¹ G. Motoyama,² Y. Uwatoko,³ S. Ban,⁴ S. Nakamura,⁴

T. Nishioka,⁵ Y. Homma,⁶ Y. Shiokawa,⁶ K. Hirota,¹ and N.K. Sato⁴

¹Neutron Sci. Lab., ISSP, University of Tokyo, Tokai, Ibaraki 319-1106, Japan

²Department of Material Science, Graduate School of Material Science, University of Hyogo, Hyogo 678-1297 Japan

³ISSP, University of Tokyo, Kashiwa 277-8581, Japan

⁴Department of Physics, Graduate School of Science, Nagoya University, Nagoya 464-8602, Japan

⁵Department of Material Science, Faculty of Science, Kochi University, Kochi 780-8520, Japan

⁶Oarai Branch, Inst. for Mater. Research, Tohoku University, Oarai, Ibaraki 311-1313, Japan

(Dated: February 8, 2020)

We report the temperature dependence of ferromagnetic Bragg peak intensities (I_B) of the superconducting ferromagnet UGe₂. When the temperature is lowered, $I_B(T)$ steeply increases below a characteristic temperature (T_X) in the ferromagnetic phase. We have found that $I_B(T)$ below T_X can be explained by a conventional Stoner model, and that a so-called Stoner gap decreases with increasing pressure and collapses in the vicinity of a critical pressure (P_X) where T_X becomes suppressed to zero. We propose a model to explain the results obtained.

PACS numbers: 65.40.-b, 71.28.+d, 71.30.+h, 71.27.+a

Since a pioneer paper by Ginzburg on the coexistence of ferromagnetism and superconductivity [1], the interplay between these two long-range orderings has been an interesting topic in solid-state physics. Superconductivity and magnetism would be antagonistic ground states, because of the competitive nature between the superconducting screening (Meissner effect) and the internal fields generated by magnetic orderings. During the last three decades, however, the discovery of a number of magnetic superconductors has allowed for a better understanding of how magnetic order and superconductivity can coexist. It is now understood that antiferromagnetism with local moments coming from rare-earth elements readily coexists with type II superconductivity. This is because whereas magnetism is connected with deeply seated $4f$ electrons, superconductivity is fundamentally related to the outermost electrons such as s , p , and d electrons.

In the case of a ferromagnetic superconductor, a trickier negotiation is needed for the coexistence. In ErRh₄B₄ [2], for example, superconductivity occurs at 8.7 K. Once the Er sublattice starts to order ferromagnetically below about 0.8 K, the superconductivity is immediately destroyed, except a very narrow coexistence region around 0.8 K. However, the magnetic structure coexisting with the superconductivity is not purely ferromagnetic but spatially modulated. The second example is ErNi₂B₂C. It was reported to exhibit a microscopic coexistence between weak ferromagnetism and superconductivity, but detailed neutron diffraction investigations indicated that the magnetism coexisting with the superconductivity is not purely ferromagnetic [3], again.

Recently, Saxena *et al.* discovered a different type of the ferromagnetic superconductor UGe₂ in which superconductivity occurs at high pressures [4]. In particular, it is surprising that the ferromagnetism may be carried by itinerant electrons homogeneously spread in the real space. This observation has renewed our interest on the interplay of ferromagnetism and superconductivity. Fig-

ure 1 shows a temperature-pressure phase diagram of UGe₂. A Curie temperature (T_{FM}) is about 52 K at ambient pressure, and monotonically decreases with increasing pressure. Then, it collapses to zero temperature at a ferromagnetic critical pressure P_{FM} (~ 1.5 GPa). In the ferromagnetic phase, there seems to be another phase transition or crossover at T_X ($\simeq 32$ K at ambient pressure). This characteristic temperature T_X also decreases with increasing pressure and becomes suppressed to zero at another critical pressure P_X ($\simeq 1.2$ GPa). It is likely that the transition at both P_X and P_{FM} is of the first order in nature [5]. Superconductivity appears in the pressure range between ~ 1.0 and ~ 1.5 GPa. Since a maximum superconducting transition tempera-

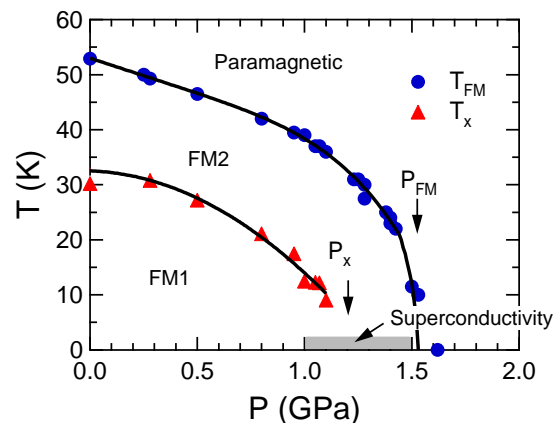


FIG. 1: Phase diagram for UGe₂ determined by our neutron diffraction measurements. The shaded region between about 1.0 and 1.5 GPa shows a superconductivity region taken from the literature [8]. The solid lines are guides to the eye. “FM1” denotes a perfectly polarized ferromagnetic state in which only majority spin bands are occupied. For “FM2” state above P_X , see the discussion in the text.

ture ($T_{SC} \sim 0.7$ K) appears at around P_X [4], we speculate that the critical point P_X can be related to the onset of the superconductivity, as was theoretically argued by Watanabe and Miyake [6] and Sandeman *et al.* [7]. Very recently, Nakane *et al.* provided a strongly supporting evidence for the speculation by means of ac magnetic susceptibility measurements [8]. However, it remains unclear what happens at P_X . In this paper, we present the temperature dependence of magnetic Bragg peak intensities under pressure by the neutron diffraction technique to reveal the nature of the transition at P_X .

Single crystals were grown by the Czochralsky pulling method using a tetra-arc furnace installed at Oarai Branch of Institute for Material Research, Tohoku University [9]. The pressure was generated using a copper-beryllium (CuBe) based piston-cylinder clamp device [10] with Fluorinert FC-75 (3M Co. Ltd., Tokyo) as a pressure transmitting medium. The low temperature pressure was determined by measurements of the change in a lattice parameter of NaCl put together with the sample. Elastic neutron scattering experiments were done on the ISSP cold neutron triple-axis spectrometer HER (C1-1) installed at JRR-3M, JAERI, Japan, with a typical configuration of energy $k_i = 1.11 \text{ \AA}^{-1}$ or 1.555 \AA^{-1} and collimations of Guide-Open-80'-80'. A cooled Be filter was placed before the sample to remove higher order contaminations. The crystals were oriented with the a -axis perpendicular to the scattering plane. Temperature was cooled down to 1.4 K using a ^4He -pumping ILL-type orange cryostat. The dc magnetization measurements were carried out using a conventional vibrating sample magnetometer (VSM) [9].

In Fig. 2 we show the pressure dependence of magnetic Bragg peak intensities $I_B(T)$ at $Q = (0,0,1)$ as a function of temperature. All data were accumulated at $k_i = 1.555 \text{ \AA}^{-1}$ in the process of increasing temperature. It is to be stressed that the obtained T -dependence in the intensities directly corresponds to that of the sample magnetization, in remarkably contrast with conventional dc magnetization measurements where a pressure cell usually includes a T -dependent component of the magnetization. While there is no apparent anomaly at 0.28 GPa, we clearly observed at 1.1 GPa a steep increase below $T_X \sim 10$ K. (In the present study, we define T_X as a maximum temperature appearing in the second derivative of the $I_B(T)$ curve with respect to T .) We note that the overall feature of the present result is consistent with the Bragg peak intensity and static magnetization data previously reported in Refs. [9, 11, 12]. At 1.23 GPa, such an anomalous behavior was not observed in accordance with $P_X \sim 1.2$ GPa.

Remembering that the neutron intensities are proportional to the square of magnetization M , we calculate the magnetic Bragg peak intensities in terms of a conventional Stoner model, which is expressed as follows (see, for example, [13]);

$$M = M_0 \{1 - \alpha \cdot T^{\frac{3}{2}} \cdot \exp(-\Delta/T)\}, \quad (1)$$

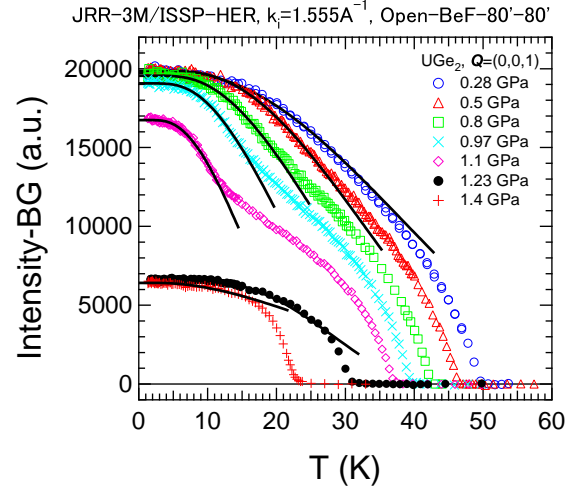


FIG. 2: Temperature dependence of the ferromagnetic Bragg peak intensities at $Q = (0,0,1)$ against the temperature T measured at various pressures. Intensities in the paramagnetic phase are subtracted from the data. Note that $P_X \sim 1.2$ GPa. The solid lines are calculated results on the basis of the Stoner model described in the text.

$$\alpha = \frac{3}{4} \sqrt{\pi} \left\{ \frac{1}{E_F} \right\}^{\frac{3}{2}}, \Delta = 2E_F \left\{ \frac{\Theta'}{E_F} - 2^{-\frac{1}{3}} \right\}, \quad (2)$$

where M_0 indicates the magnetization at zero temperature, Δ a so-called Stoner gap, E_F a Fermi energy, and Θ' is a molecular field coefficient. The results are shown in Fig. 2 by the solid lines. Interestingly, we find extraordinarily good accordance between the experiment and the calculation. This suggests that the decrease of the magnetization at very low temperatures is mainly caused by the electron-hole excitation in quasiparticle bands.

From the least square fitting, we estimate a set of parameters α and Δ in eq. (1), which further enables us to evaluate E_F and Θ' using eq. (2). First we concentrate on the pressure region below P_X . In Fig. 3 (a) we show Δ and Θ' together with T_X , each of which is normalized to a respective value at ambient pressure. It is interesting to note that these quantities seem to lie on a single line, suggesting that the characteristic temperature of the unknown origin, T_X , is related to the Stoner gap Δ (equivalently Θ') in the quasiparticle band.

In Fig. 3 (b) we plot a ratio of Θ'/E_F against P . According to the Stoner model, if the ratio is greater than $2^{-\frac{1}{3}} (\sim 0.793)$, then the system is in a perfectly polarized ferromagnetic state, where only a majority spin band is occupied. When the ratio lies between $2/3$ and $2^{-\frac{1}{3}}$, an imperfectly polarized ferromagnetic state occurs, where a minority spin band becomes to be partially occupied by quasiparticles. Further in the case that the ratio is smaller than $2/3$, the system is paramagnetic. As seen in the figure, our analysis indicates that the perfectly polarized state is realized below P_X in UGe_2 . Actually, band structure calculations indicate that Fermi surfaces

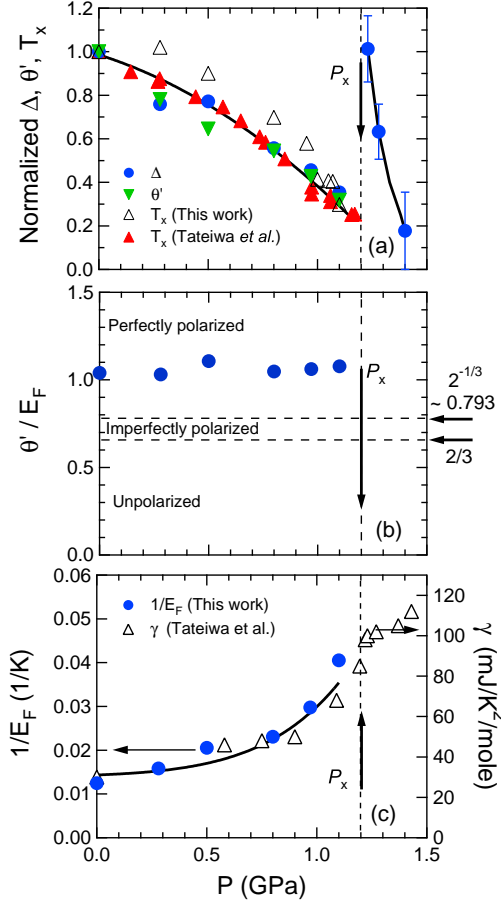


FIG. 3: Pressure dependence of the obtained parameters from the Stoner model. The solid lines are guides to the eye. (a) Δ , Θ' , and T_X plotted are normalized with respect to a respective ambient pressure value; $\Delta = 39.5$ K, $\Theta' = 83.4$ K, and $T_X = 30.2$ K. We also plot T_X taken from Ref. [14]. (b) Ratio of Θ'/E_F is plotted against P below P_X . Note that the pressure region for $P < P_X$ corresponds to the perfectly polarized state in the Stoner model, i.e., $\Theta'/E_F > 2^{-1/3}$. For the state above P_X , see the discussion in the text. (c) Inverse Fermi energy $1/E_F$ is plotted against P below P_X , together with an electronic specific heat coefficient γ taken from Ref. [14].

have a predominantly majority spin character [15, 16], providing a supporting evidence for our model.

We plot $1/E_F$ vs. P in Fig. 3 (c). Assuming that $E_F D(E_F)$ is a constant value independent of the pressure, where $D(E_F)$ denotes a density of states at E_F , then $1/E_F$ is proportional to $D(E_F)$, and hence to an electronic specific heat coefficient γ . As clearly seen in Fig. 3 (c), we find that $1/E_F = c\gamma$, where c is a constant independent of P and γ is an observed value reported by Tateiwa *et al.* [14]. (We note that while it seems very difficult to deduce reliable information of the superconductivity from the specific heat experiments because of a small anomaly at T_{SC} , it is rather easy to reveal normal properties such as the γ value which is as large as several

tens of mJ/K².) This coincidence between $1/E_F$ and γ strongly supports the applicability of the present model to UGe₂.

Figure 4 (a) shows the dc magnetization $M(T)$ at 1.18 GPa ($< P_X$) as a function of temperature. (The magnetization of the pressure cell was subtracted from the total measured magnetization.) The external magnetic field H_{ext} is applied along the magnetization easy a -axis. We observed a step-like increase in the $M(T)$ curve at lower fields, similarly to that in the $I_B(T)$ curve. As is already known, T_X increases with H_{ext} [5, 8]. We stress that the static magnetization can also be well described by the Stoner model (see dotted lines). In Fig. 4 (b) we plot Δ as a function of H_{ext} , which was obtained in the same manner as above. It is found that Δ increases almost linearly with H_{ext} , as shown by the broken line. This is highly expected from the Stoner model: In the Stoner model, the gap in the quasiparticle band should increase with the magnetic field due to the Zeeman effect as follows,

$$\Delta(H) = \Delta + 2g\mu_B SH. \quad (3)$$

Here, Δ is a value at zero magnetic field, i.e., $\Delta(H = 0)$, g and S denote a g -factor and the magnitude of the quasiparticle spin, respectively, and μ_B is the Bohr magneton. Indeed, the value of $\Delta \simeq 12$ K estimated from the extrapolation to the zero field is consistent with a value obtained from the Bragg peak intensity (at $H = 0$) mentioned above. A set of parameters, $g = 6/7$ and $S = 5/2$ corresponding to an f electron, produces better agreement between the observation and the calculation than another set of parameters, $g = 2$ and $S = 1/2$ for a free electron. This may reflect that the heavy quasiparticle arises from f electrons.

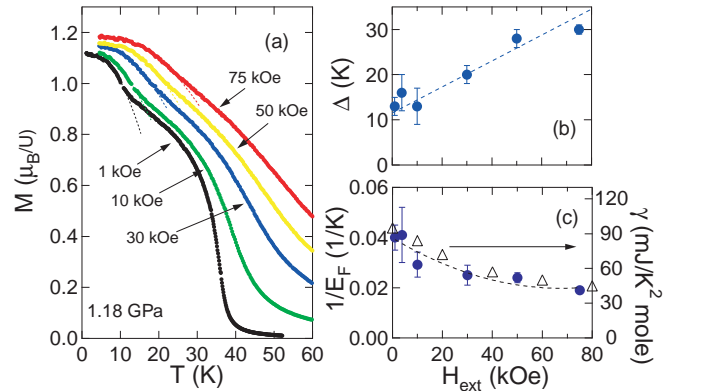


FIG. 4: (a) Temperature dependence of the static magnetization at 1.18 GPa under various magnetic fields along the magnetization easy a -axis. (b) Stoner gap Δ is plotted as a function of the external magnetic field H_{ext} . (c) Inverse Fermi energy $1/E_F$ is plotted together with the electronic specific heat coefficient γ measured at 1.15 GPa taken from Ref. [17]. Note that $1/E_F$, which is proportional to the density of states at E_F , agrees well with the observed γ value.

The least square fitting of the $M(T)$ data to the Stoner model gives $1/E_F$ as a function of H_{ext} at 1.18 GPa, the results being plotted in Fig. 4 (c). It is interesting to compare it with the γ value directly deduced from the specific heat experiment [17]. We find again the good accordance between $1/E_F$ and γ . Here, we emphasize that we employed the same scale factor c between $1/E_F$ and γ as that for Fig. 3 (c), meaning that there is no adjustable parameter in Fig. 4 (c) at all. This proves the validity of our model, again.

Now we return to the data of 1.23 GPa ($> P_X$) given in Fig. 2. It is to be noted that the intensity is almost T -independent below about 11 K, in contrast to the rather steep variation at 1.1 GPa. Correspondingly, the fitting yields a sudden jump of Δ from about 14 K at 1.1 GPa to $40 (\pm 6)$ K at 1.23 GPa, reflecting the first-order transition at P_X . Furthermore, the fitting of $P = 1.28$ and 1.40 GPa data to the same equation produces $\Delta = 25 (\pm 5)$ and $7 (\pm 7)$ K, respectively, indicating that Δ decreases monotonically with further increasing P above P_X and seems to tend toward zero in the vicinity of the ferromagnetic critical pressure P_{FM} (see Fig. 3 (a)).

To explain the results obtained at the both sides of P_X in a unified way, we propose the following model: The magnetization is described by the summation of two components, $M_{tot}(T) = M_1(T) + M_2(T)$, which are characterized by the gap Δ_1 and Δ_2 , respectively. The P -dependence of the gap in Fig. 3 (a) leads us to assume that Δ_1 (Δ_2) is a decreasing function of P and vanishes in the vicinity of P_X (P_{FM}), and that Δ_2 is much greater than Δ_1 below P_X . This assumption implies that $M_2(T)$ is weakly T -dependent at low temperatures in the perfectly polarized region, so that the inclusion of the second component into the analysis will not change so much the results obtained above. It seems reasonable to assign Δ_1 to the aforementioned Stoner gap, and then the question to be addressed is what Δ_2 implies. We consider two possibilities, (i) another Stoner gap and (ii) an anisotropy gap of ferromagnetic spin waves. (The spin wave theory gives the same expression as eq. (1) for a uniaxial ferro-

magnet [18].) Unfortunately, it is impossible to conclude from the present analysis which is realized in UGe₂. However, we speculate that the strong anisotropy remaining above P_X [20] favors the latter possibility, which requires further investigation.

The former possibility means that the ferromagnetism can be fully understood within the framework of the band picture over the entire P and T region, while the latter may indicate the presence of localized $5f$ electrons. According to Yaouanc *et al.*, positive muon spin relaxation measurements at ambient pressure suggested that UGe₂ is a dual system where an electronic subset of itinerant states coexists with the subset of localized electrons responsible for the well-known bulk magnetic properties [21], similarly to the superconducting antiferromagnet UPd₂Al₃ [22]. It may be interesting to reinvestigate the ferromagnetic properties of UGe₂ in view of the dual nature of $5f$ electrons.

In conclusion, we investigated the magnetization of the superconducting ferromagnet UGe₂ by the neutron diffraction technique together with the dc magnetization measurements under pressure. We found that the temperature dependence of the magnetization is well explained by the Stoner model, and that the Stoner gap Δ decreases with increasing pressure and collapses in the vicinity of the critical pressure (P_X) where the superconducting transition temperature displays a maximum. These results imply that the perfectly polarized state in which the heavy quasiparticles occupy the majority spin band is realized below P_X .

Acknowledgments

We thank K. Miyake and S. Watanabe for useful discussions. This work was supported by a Grant-in-Aid from the Ministry of Education, Culture, Sports, Science and Technology, Japan. NKS also thanks Daiko Foundation for partial financial support.

-
- [1] V.L. Ginzburg, Sov. Phys. JETP **4** (1957) 153.
 - [2] M. Tachiki, "Progress in Theory of Magnetism" Edited by T. Moriya and J. Kanamori (1983, Syokabo, Tokyo) p.114. (in Japanese).
 - [3] H. Kawano-Furukawa *et al.*, Phys. Rev. **B 65** (2002) 180508.
 - [4] S.S. Saxena *et al.*, Nature (London) **406** (2000) 587.
 - [5] C. Pfleiderer and A. D. Huxley, Phys. Rev. Lett. **89** (2002) 147005.
 - [6] S. Watanabe and K. Miyake, J. Phys. Soc. Jpn. **71** (2002) 2489.
 - [7] K.G. Sandeman *et al.*, Phys. Rev. Lett. **90** (2003) 167005.
 - [8] H. Nakane *et al.*, to appear in J. Phys. Soc. Jpn. **74** (2005) 855.
 - [9] G. Motoyama *et al.*, Phys. Rev. **B 65** (2002) 020510.
 - [10] For example, I. Umehara *et al.*, J. Mag. Mag. Mat. **272-76** (2004) 2301.
 - [11] A. Huxley *et al.*, Phys. Rev. **B 63** (2001) 144519.
 - [12] N. Tateiwa *et al.*, J. Phys. Soc. Jpn. **70** (2001) 2876.
 - [13] E.C. Stoner, Proc. Roy. Soc. **A 165** (1938) 372.
 - [14] N. Tateiwa *et al.*, J. Phys. Cond. Matter **13** (2001) L17.
 - [15] H. Yamagami, J. Phys. Cond. Matt. **15** (2003) S2271.
 - [16] A.B. Shick and W.E. Pickett, Phys. Rev. Lett. **63** (2001) 300.
 - [17] N. Tateiwa *et al.*, Physica **B 312-313** (2002) 109.
 - [18] A.I. Akhiezer *et al.*, "Spin waves" Edited by S. Doniach (1968, North-Holland, New York) p. 204.
 - [19] C. Geibel *et al.*, Z. Phys. **84** (1991) 1.
 - [20] A. Huxley *et al.*, J. Phys.: Condens. Matter. **15** (2003) S1945.
 - [21] A. Yaouanc *et al.*, Phys. Rev. Lett. **89** (2002) 147001.
 - [22] N.K. Sato *et al.*, Nature (London) **410** (2001) 340.